Journal of Geophysical Research: Space Physics

Supporting Information for

EMIC wave parameterization in the long-term VERB code simulation

A.Y. Drozdov[1], Y.Y. Shprits[2,3,1], M. E. Usanova[4], N. Aseev[2], A. Kellerman[1], H. Zhu[5]

1 Department of Earth, Planetary and Space Sciences, University of California Los Angeles, Los Angeles, California, USA
2 Helmholtz Centre Potsdam, GFZ German Research Centre for Geosciences, Telegrafenberg, Potsdam, Germany
3 Institute for Physics and Astronomy, University of Potsdam, Germany
4 Laboratory for Atmospheric and Space Physics, University of Colorado Boulder, Boulder, Colorado, USA
5 William B. Hanson Center for Space Sciences, Department of Physics, University of Texas at Dallas, Richardson, Texas, USA

Contents of this file

Figures S1 to S12

Introduction

As discussed in the manuscript, we consider several parameters of the EMIC wave presence. Several simulations show similar low MAE. For each of the simulations, we compare the evolution of the electron fluxes and the pitch angle distribution with the observations and the simulation without EMIC waves. The comparison is presented on the supplementary figures.

Figures S1-S5 are similar to Figure A2 and show the evolution of the electron flux from observations, simulation without EMIC waves and selected simulations with EMIC waves. Each figure corresponds to the single parameter of EMIC wave presence from Table 1.

Figure S1 shows the case of EMIC wave presence parameterized by Kp. The simulations are similar except for the electron flux decay after 8 October 2012. The simulation in Figure S1e shows better agreement with the observations and corresponds to simulation with minimum MAE in Figure A1a.

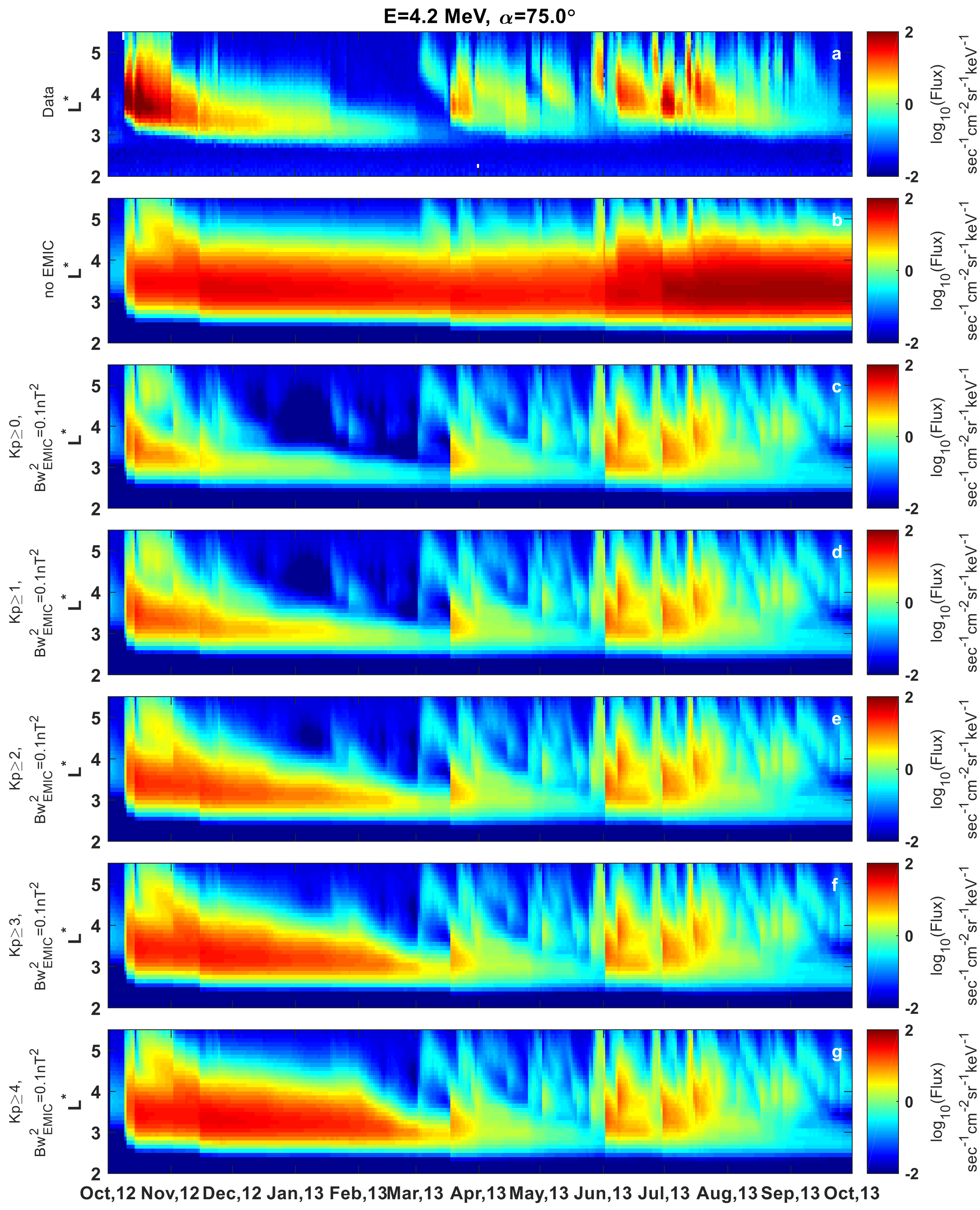

Figure S1. Evolution of the 4.2 MeV electron fluxes at the pitch-angle of 75° similar to Figure A2. c-g) simulations with different Kp index EMIC wave parameterizations.

Figure S2 shows the case of EMIC wave presence parameterized by Dst. The simulations in Figures S2e-g show the overestimated flux at the end of the simulations. The simulations in Figure S2c and S2d are similar. The simulations in Figure S2c show slightly better agreement than the simulation in Figure S2d due to the flux level at the end of the simulation and after the 8 October 2012 storm.

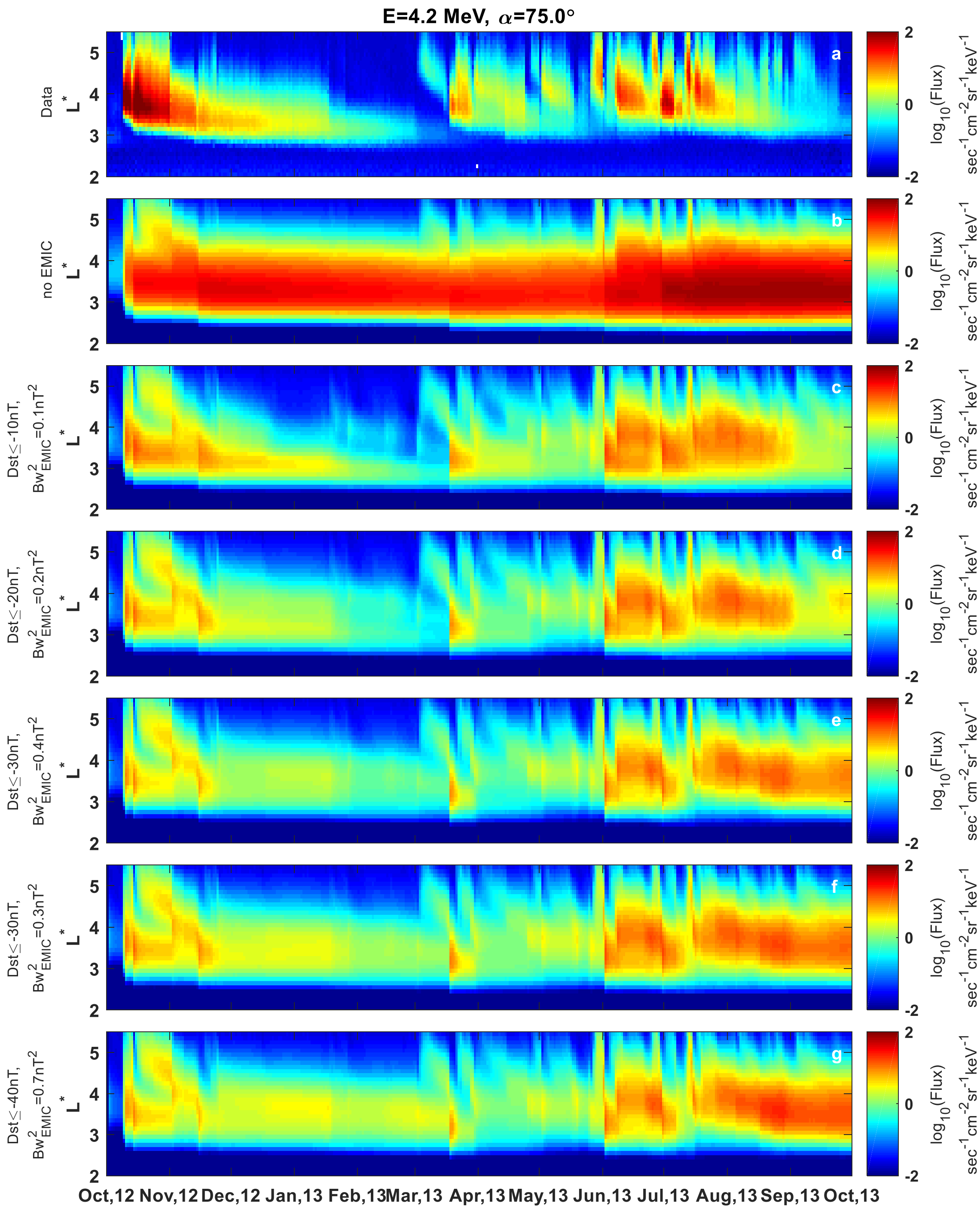

Figure S2. Evolution of the 4.2 MeV electron fluxes at the pitch-angle of 75° similar to Figure A2. c-g) simulations with different Dst index EMIC wave parameterizations.

Figure S3 shows the case of EMIC wave presence parameterized by V_{sw}. The simulations in Figures S2e-g show unrealistic dynamics during October 2012. Despite this, the simulation in Figure S2c does not reproduce the dynamics during October 2012, but it provides the better agreement with observations and corresponds to the minimum in Figure A1c.

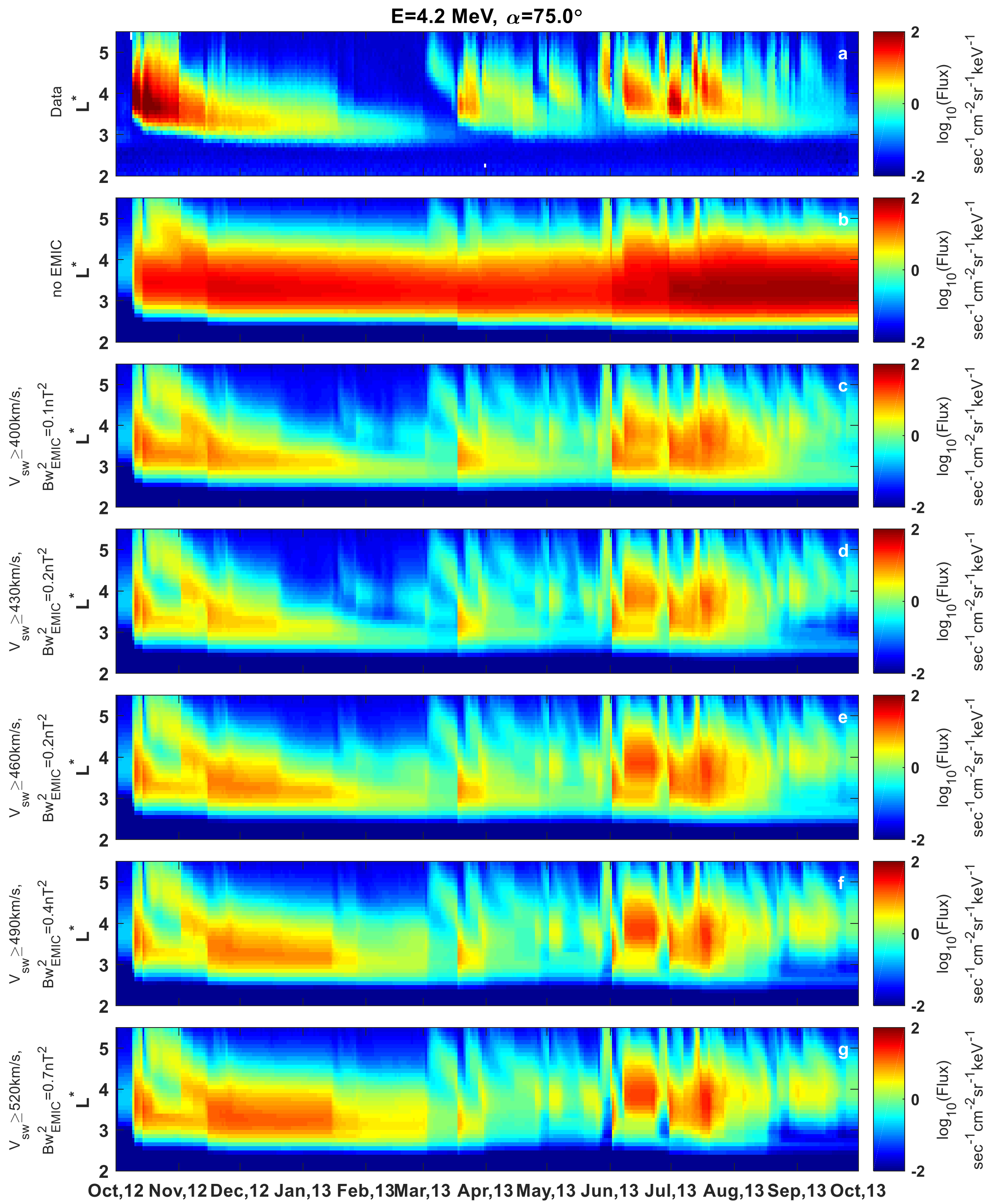

Figure S3. Evolution of the 4.2 MeV electron fluxes at the pitch-angle of 75° similar to Figure A2. c-g) simulations with different solar wind speed EMIC wave parameterizations.

Figure S4 shows the case of EMIC wave presence parameterized by P_{dyn}. The simulations in Figures S4c-g are very similar. Simulations in Figure S3e and S3g slightly overestimate the flux level at the end of the simulation. Simulations in Figures S4c-e better reproduce the level of the flux decay after 8 October 2012. Simulations in Figures S4e-g better reproduce the flux dropout in January 2013. The simulation in Figure S4e corresponds to the minimum in Figure A1d.

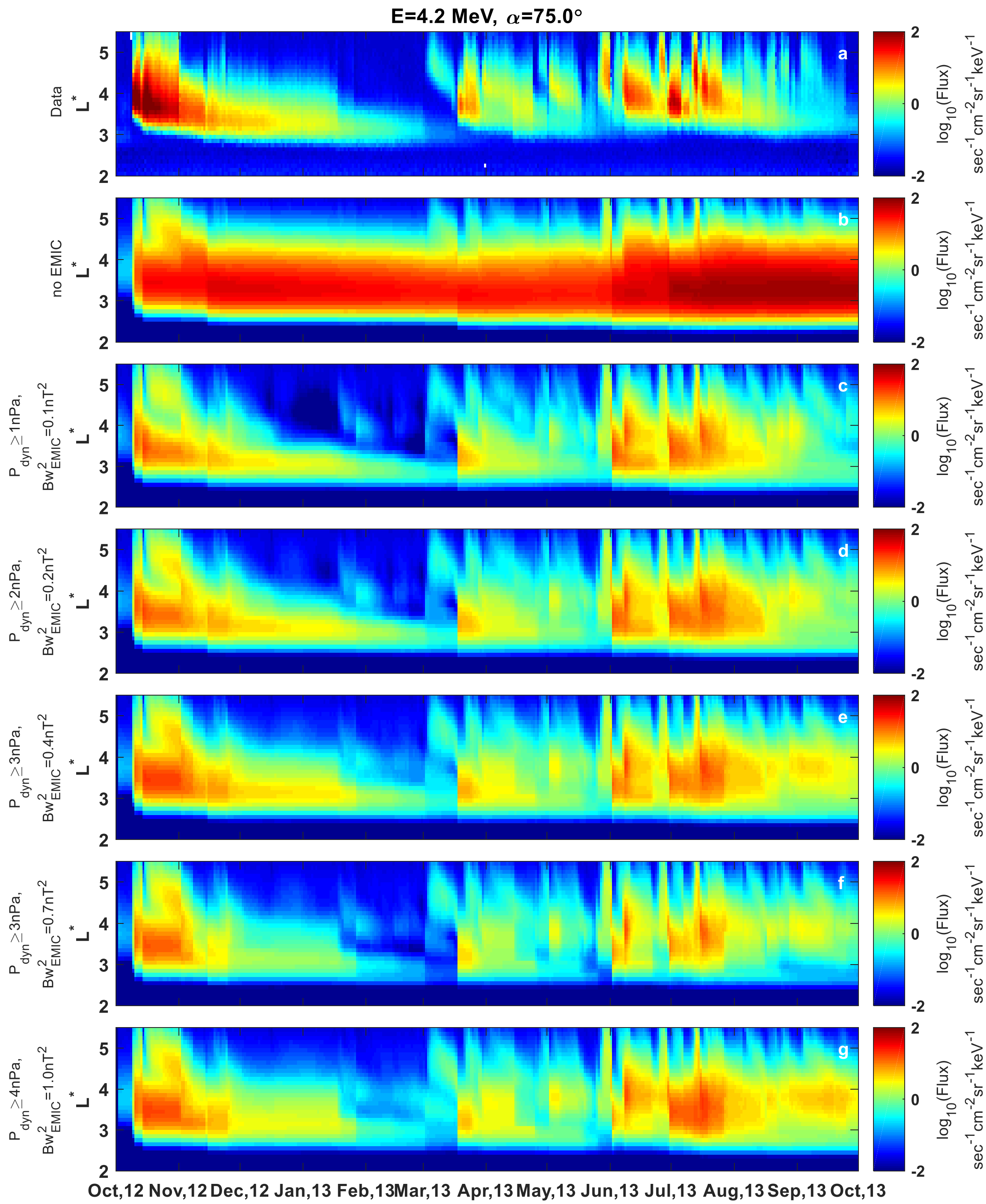

Figure S4. Evolution of the 4.2 MeV electron fluxes at the pitch-angle of 75° similar to Figure A2. c-g) Simulations with different solar wind pressure EMIC wave parameterizations.

Figure S5 shows the case of EMIC wave presence parameterized by AE. The simulations in Figures S5c-g are very similar. The simulations in Figures S5e-g provide a wider belt after the 8 October 2012 storm in comparison to the observations. The simulations in Figures S5c-d are almost identical, and the simulations in Figure S5d correspond to the minimum in Figure A1e.

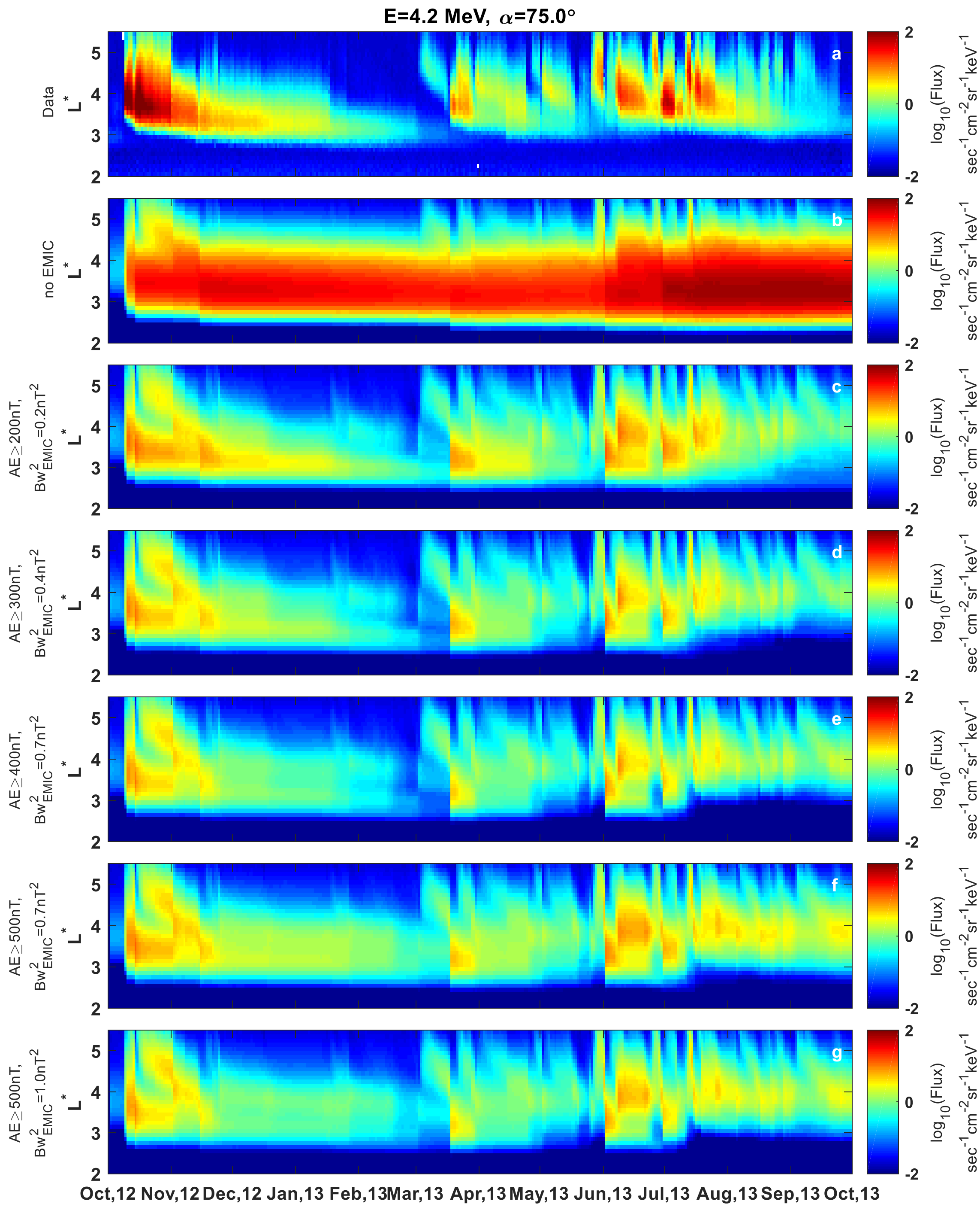

Figure S5. Evolution of the 4.2 MeV electron fluxes at the pitch-angle of 75° similar to Figure A2. c-g) Simulations with AE index EMIC wave parameterizations.

Figures S6-S10 are similar to Figure A3 and show the pitch-angle distribution from observations, simulation without EMIC waves, and selected simulations with EMIC waves. Each figure corresponds to the single parameter of EMIC wave presence.

Figure S6 shows the case of EMIC wave presence parameterized by Kp. None of the simulations reproduce the observed pitch-angle distribution. The preference can be given to the simulations in Figures S6d and S6e, since the flux before the rapid depletion on 1 November 2012 and the time of the depletion is closer to the observations in comparison to other simulations in Figure S6. In combination with the analysis of Figures S1 and S6, the simulation that corresponds to the minimum of MAE from Figure A1a can be selected for comparison with other simulations with different EMIC wave presence parameters.

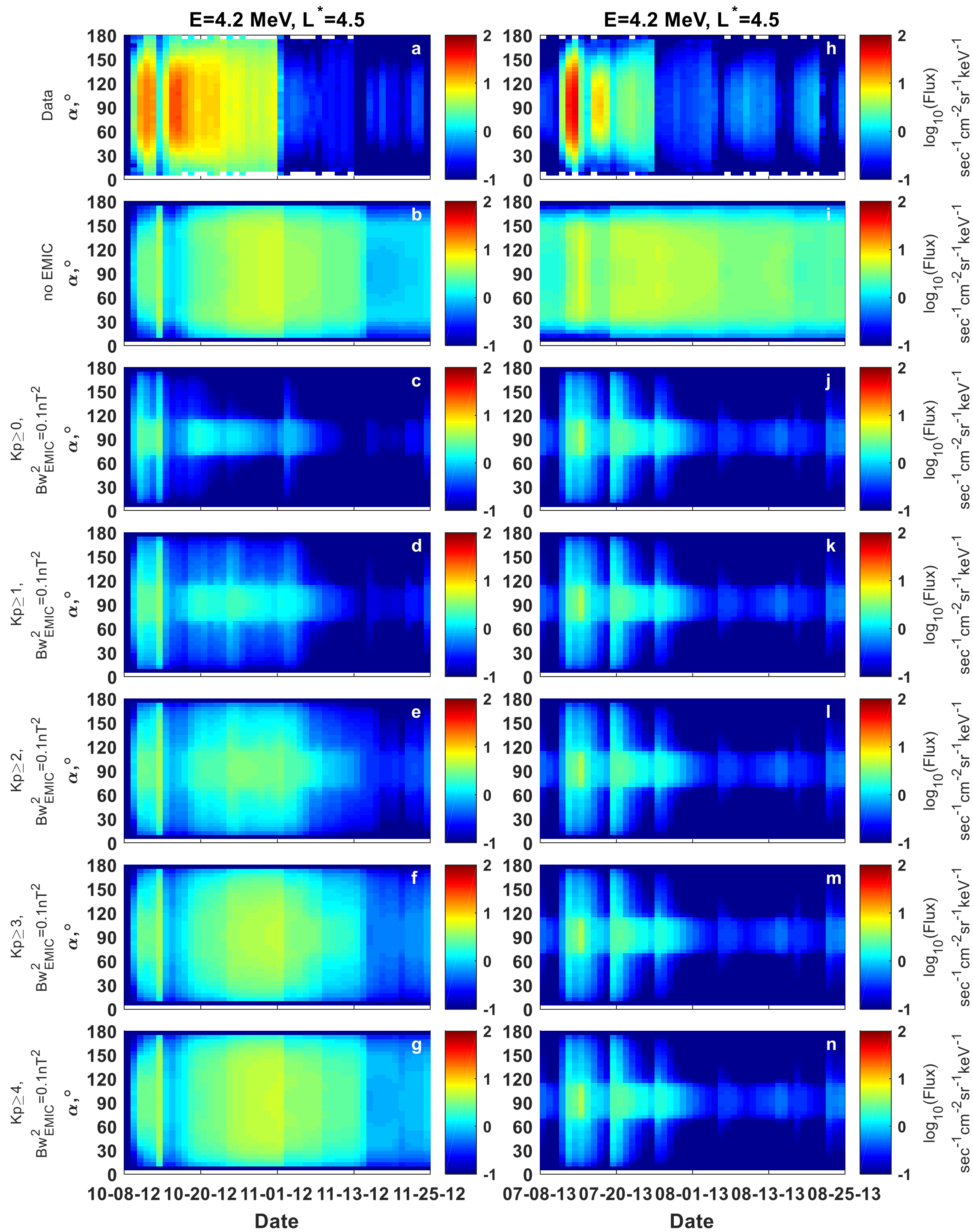

Figure S6. The pitch-angle distribution evolution of 4.2 MeV electron fluxes at L*=4.5 similar to Figure A3. c-g and j-n) simulations with different Kp index EMIC wave parameterizations.

Figure S7 shows the case of EMIC wave presence parameterized by Dst. All simulations with EMIC waves provide reasonable agreement with the observations; however, there are several uncertainties. The flux level in Figure S7n is larger than in the observation, and pitch-angle distribution is wider. In a comparison between simulations in Figure S7c and S7d, the pitch-angle distribution starting on 18 October 2012 is more narrow in Figure S7c. This dynamic is not shown by the observations. A combination of analyses of Figures S2 and S7 show that the simulation corresponding to the minimum of MAE from Figure A1b can be selected for comparison with other simulations with different EMIC wave presence parameters.

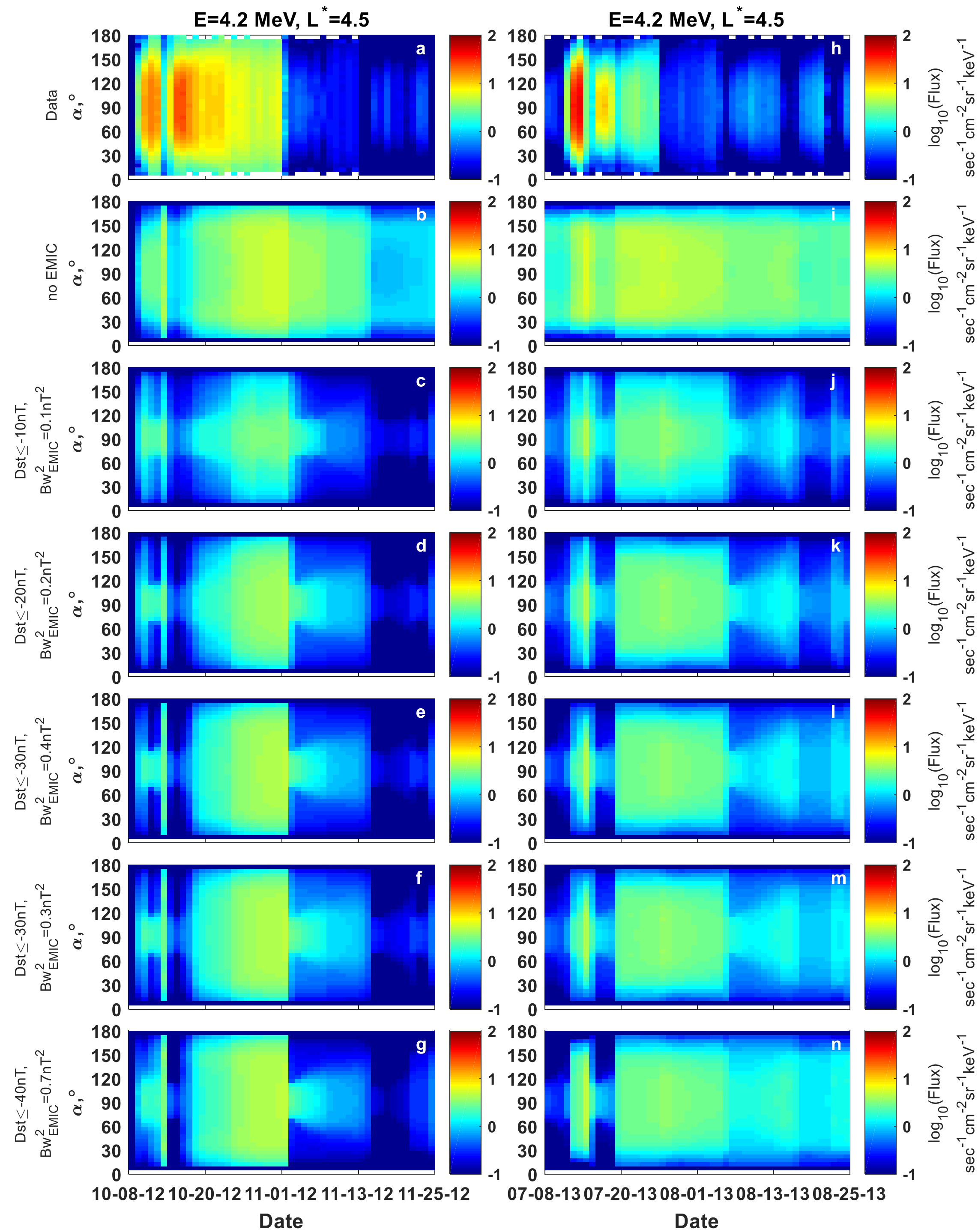

Figure S7. The pitch-angle distribution evolution of 4.2 MeV electron fluxes at L*=4.5 similar to Figure A3. c-g and j-n) simulations with different Dst index EMIC wave parameterizations.

Figure S8 shows the case of EMIC wave presence parameterized by V_{sw}. All simulations with EMIC waves are very similar, and none of the simulations reproduce the pitch-angle distribution. This makes it difficult to prefer one simulation to another. A combination of analyses of Figures S3 and S8 show that the simulation corresponding to the minimum of MAE from Figure A1c can be selected for comparison with other simulations with different EMIC wave presence parameters.

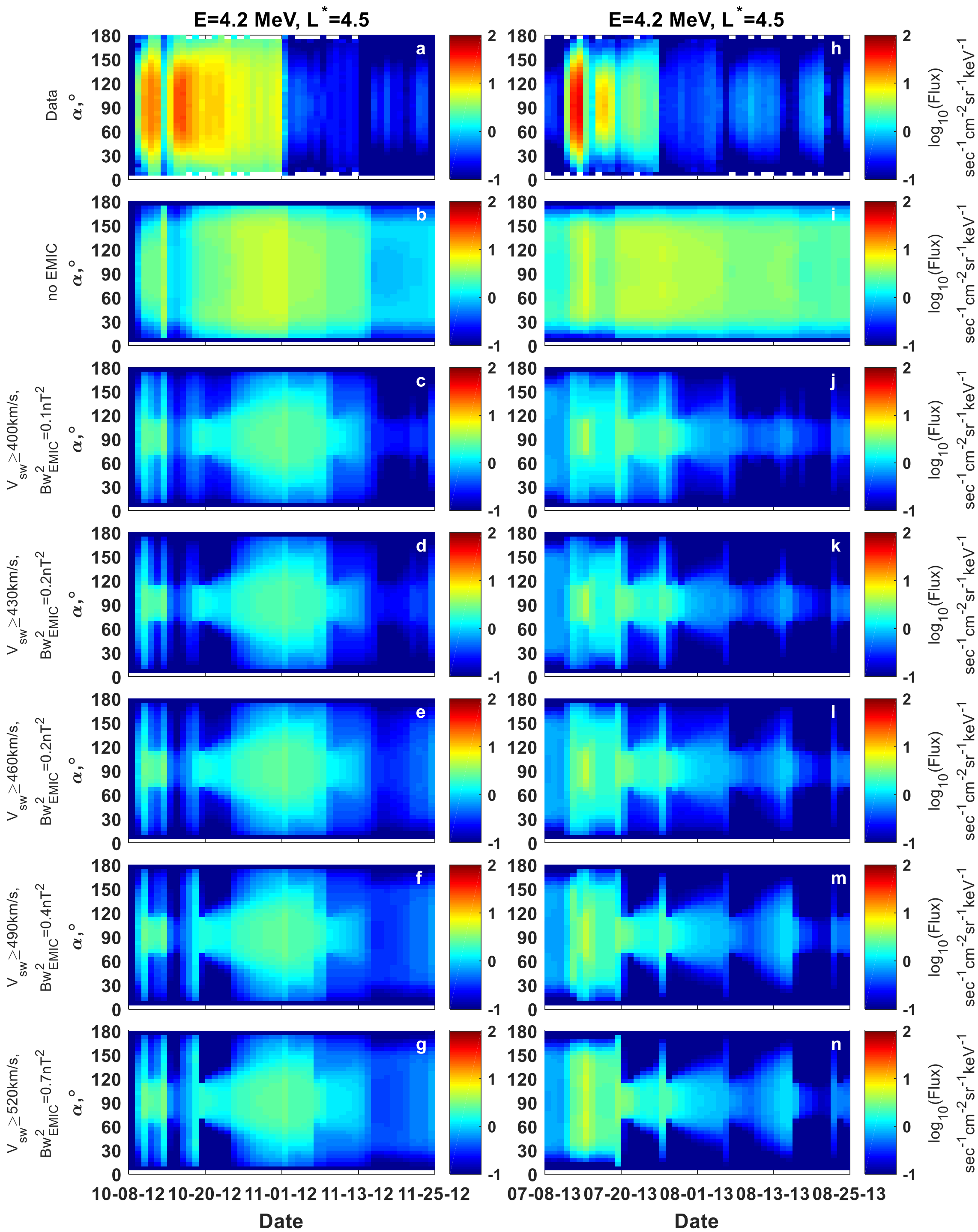

Figure S8. The pitch-angle distribution evolution of 4.2 MeV electron fluxes at L*=4.5 similar to Figure A3. c-g and j-n) simulations with different solar wind speed EMIC wave parameterizations.

Figure S9 shows the case of EMIC wave presence parameterized by P_{dyn}. All simulations with EMIC waves provide reasonable agreement with the observations except for the simulation in Figure S9c, S9j. The flux level in Figure S7j significantly underestimates the observations. The simulations in Figure S9d provide noticeable narrowing of pitch-angle distribution after 19 October 2012, which is not seen in observations. A combination of analyses of Figures S4 and S9 show that the simulation corresponding to the minimum of MAE from Figure A1d can be selected for comparison with other simulations with different EMIC wave presence parameters.

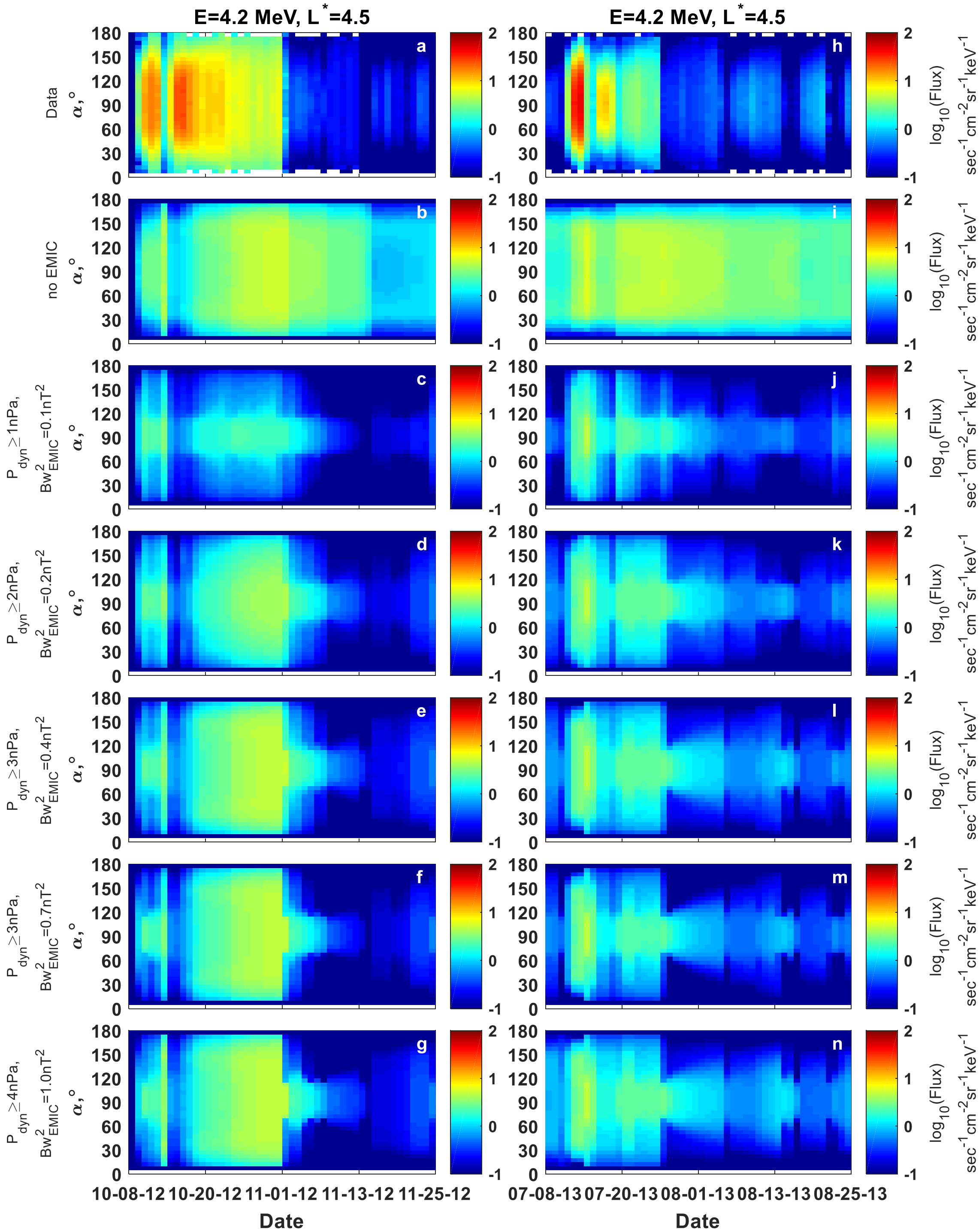

Figure S9. The pitch-angle distribution evolution of 4.2 MeV electron fluxes at L*=4.5 similar to Figure A3. c-g and j-n) simulations with different solar wind pressure EMIC wave parameterizations.

Figure S10 shows the case of EMIC wave presence parameterized by AE. All simulations with EMIC waves provide reasonable agreement with the observations. The simulations in Figure S10c provide noticeable narrowing of pitch-angle distribution after 19 October 2012, which is not seen in observations. A combination of analyses of Figures S5 and S10 show that the simulation corresponding to the minimum of MAE from Figure A1e can be selected for comparison with other simulations with different EMIC wave presence parameters.

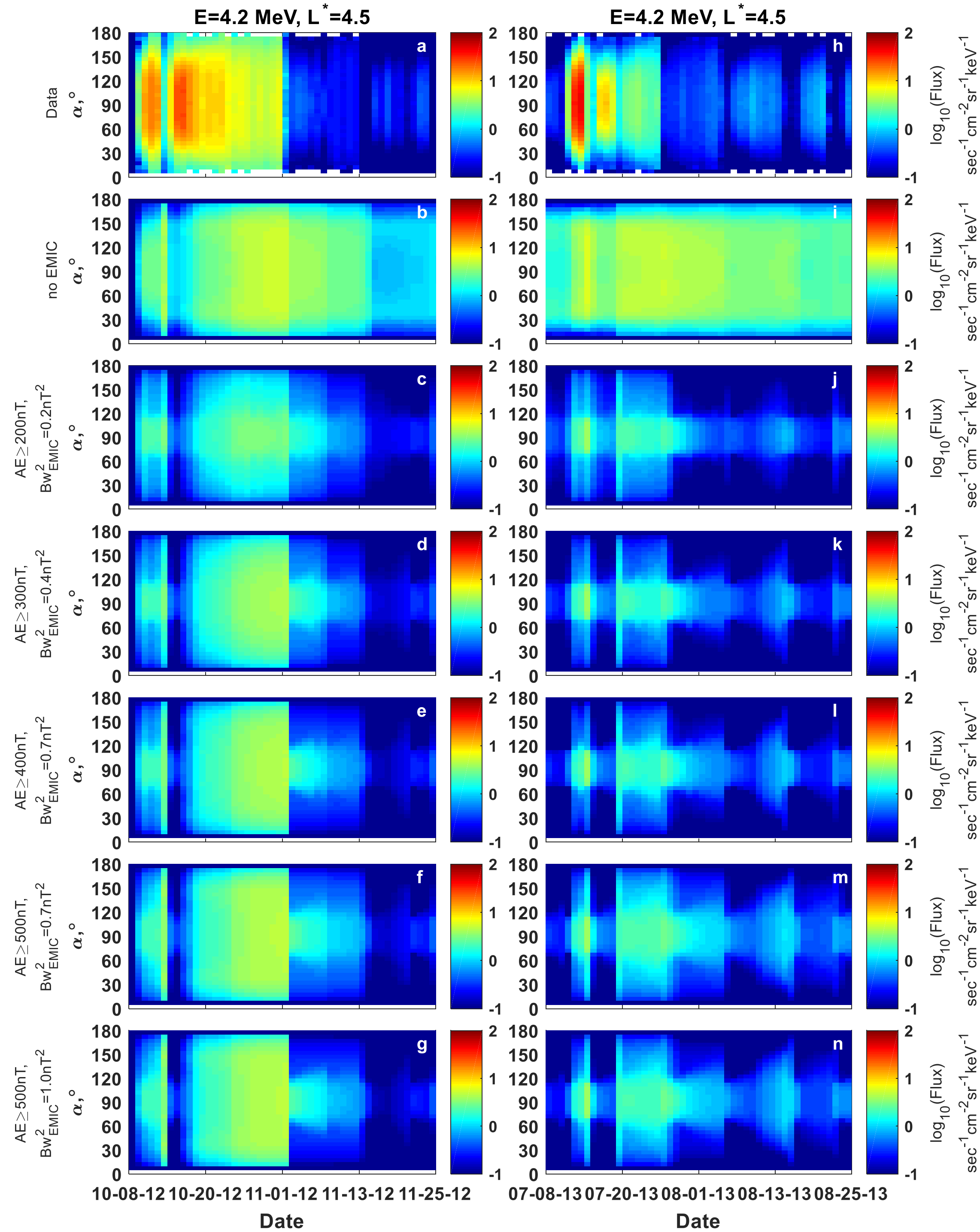

Figure S10. The pitch-angle distribution evolution of 4.2 MeV electron fluxes at L*=4.5 similar to Figure A3. c-g and j-n) simulations with different AE index EMIC wave parameterizations.

Figure S11 is similar to Figure 2, but shows the relativistic electron population. Simulations with and without EMIC waves are practically indistinguishable and provide reasonable agreement with the observations.

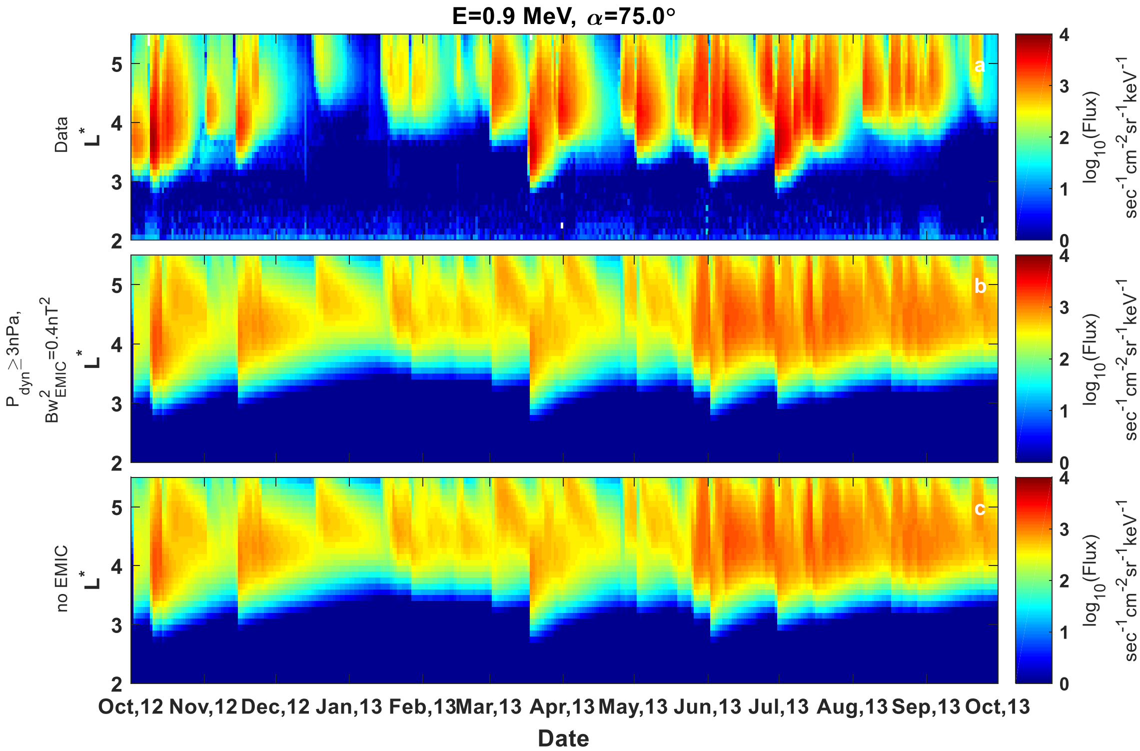

Figure S11. Evolution of the 0.9 MeV electron fluxes at the pitch-angle of 75° similar to Figure 2. a) MagEIS observations, on the simulation grid.

Figure S12 is similar to Figure 5, but as in Figure S11, it shows the relativistic electrons population. Simulations with and without EMIC waves are practically indistinguishable. However, despite good agreement between modeled flux evolution and the observations (Figure S11), the pitch-angle distribution is not accurately reproduced. This can be related to inaccurate modeling of the plasmapause location which defines the presence of the hiss and chorus waves. The inaccurate balance of different waves can lead to the inaccurate pitch angle distribution in the long-term modeling. Accurate representation of the magnetic field, plasma density, wave spectral properties and their amplitude and latitude distributions and other parameters can improve the simulation results and will be a subject of future research.

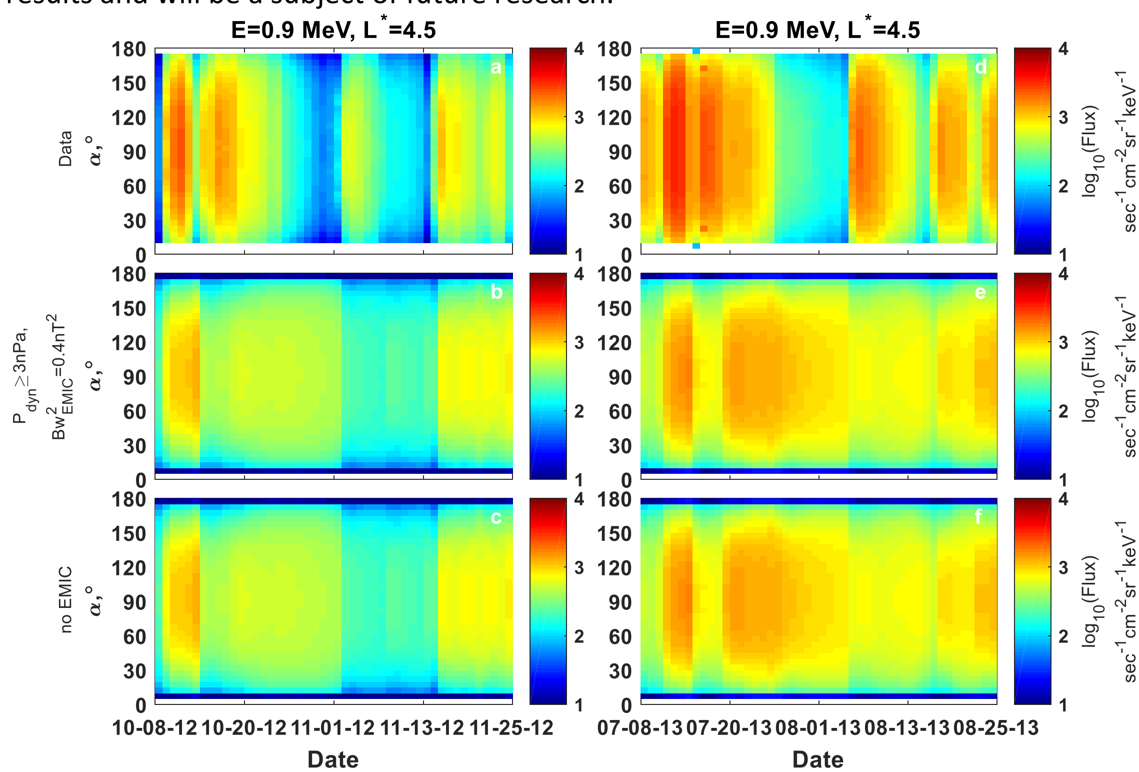

Figure S12. The pitch-angle distribution evolution of 0.9 MeV electron fluxes at L*=4.5 similar to Figure 3. a, d) MagEIS observations, on the simulation grid.